GROWSCREEN-Rhizo is a novel phenotyping robot enabling simultaneous measurements of root and shoot growth for plants grown in soil-filled rhizotrons

Running title:
Phenotyping root system architecture

Kerstin A. Nagel[1], Alexander Putz[1], Frank Gilmer[1,2], Kathrin Heinz[1], Andreas Fischbach[1], Johannes Pfeifer[1], Marc Faget[1], Stephan Bloßfeld[1], Michaela Ernst[1], Chryssa Dimaki[1], Bernd Kastenholz[1], Ann-Katrin Kleinert[1], Anna Galinski[1], Hanno Scharr[1], Fabio Fiorani[1], Ulrich Schurr[1]

Institute of origin:
[1] Institute of Bio- and Geosciences, IBG-2: Plant Sciences, Forschungszentrum Jülich GmbH, 52425 Jülich, Germany
[2] present address: BASF SE, 67117 Limburgerhof, Germany

Corresponding author:
Kerstin A. Nagel; Institute of Bio- and Geosciences, IBG-2: Plant Sciences, Forschungszentrum Jülich GmbH, 52425 Jülich, Germany; Tel: +49 2461 619113; Fax: +49 2461 612492; email: k.nagel@fz-juelich.de

Key words:
root system architecture, heritability, root traits, robotised, imaging, soil strength

Abstract

Root systems play an essential role in ensuring plant productivity. Experiments conducted in controlled environments and simulation models suggest that root geometry and responses of root architecture to environmental factors should be studied as a priority. However, compared with aboveground plant organs, roots are not easily accessible by non-invasive analyses and field research is still based almost completely on manual, destructive methods. Contributing to reducing the gap between lab and field experiments, we present a novel phenotyping system (GROWSCREEN-Rhizo) which is capable of automatically imaging roots and shoots of plants grown in soil-filled rhizotrons (up to a volume of ca. 18 L) with an throughput of 60 rhizotrons per hour. Analysis of plants grown in this setup is restricted to certain plant size (up to a shoot height of 80 cm and root system depth of 90 cm). We performed validation experiments using six different species and, for barley and maize, we studied the effect of moderate soil compaction which is a relevant factor in the field. First, we found that the portion of root systems which is visible through the rhizotrons' transparent plate is representative of the total root system. The percentage of visible roots decreases with increasing average root diameter of the plant species studied and depends, to some extent, on environmental conditions. Second, we could measure relatively minor changes in root system architecture induced by a moderate increase in soil compaction. Taken together, these findings demonstrate the good potential of this methodology to characterise root geometry and temporal growth responses with relatively high spatial accuracy and resolution for both monocotyledonous and dicotyledonous species. Our prototype will allow the design of high-throughput screening methodologies simulating environmental scenarios that are relevant in the field and will support breeding efforts towards improved resource use efficiency and stability of crop yields.

Introduction

Plant roots provide key functions encompassing anchorage to the substrate, absorption of water and nutrients, storage, hormone production for coordinated plant development, and communication with biotic and abiotic environment. The overall geometry of root systems and the architectural changes in response to environmental challenges play an essential role in growth and development, as well as in determining plant performance, productivity, and fitness (Lynch 1995; Hammer *et al.* 2009). However, due to difficulties in observing and quantifying roots in soil and, consequently, interpreting data, dynamic changes in root systems' architecture are less characterised compared to those occurring in the phyllosphere (Herder *et al.* 2010). In the past, breeding for new varieties with higher yield has mainly focused on optimising shoot biomass accumulation, geometry, and function (Gonzalez *et al.* 2009; Xing and Zhang 2010). Recent simulations suggest that the contribution of roots and root system architecture to enhancing yield has been underestimated (Hammer *et al.* 2009). The modelling approach of Hammer *et al.* (2009) indicated that the continuous increase in yield of maize in the U.S. Corn Belt over the past 70 years was directly influenced by modifications in geometry and function of root system architecture. Interestingly, Manschadi *et al.* (2006) found that the angle at which seminal wheat roots grow affects whole root system architecture and, consequently, water extraction capacity from the soil and plant productivity under water-deficit conditions. These examples highlight that a better understanding of root system structure and function is critical to improve resource use efficiency of major crops, especially under unfavourable environmental scenarios. These include not only water scarceness, but also low soil fertility and increasing salinity as well as erosion and soil degradation. Non-invasive, high-throughput phenotyping methods of root systems are indispensable for identifying genotypes with specific root system architecture resulting in increased ability to adapt plant development to changing environmental conditions. Novel technologies are required to characterise the complexity of root systems automatically to assist in identifying heritable root traits. Selection for specific traits based on integration of molecular-mechanistic knowledge with accurate measurements of plant performance could be even more productive in breeding processes than conventional field screening (Lynch 2007; Passioura 2010).

Due to practical reasons, phenotyping of root system architecture under field conditions is challenging and still relies on traditional methods, e.g., manual measurements or visual estimations (De Smet *et al.* 2012). Roots have to be harvested destructively by labour-intensive excavation processes. Remarkably, however, dedicated and trained teams could visually score root traits of excavated adult maize plants within a few minutes (Trachsel *et al.* 2011). Non-destructive measurements of roots at frequent time intervals in the field are practicable by using mini-rhizotron tubes inserted in the soil (Gregory 1979; Johnson *et al.* 2001). However, the analysis of whole root systems is not feasible because only roots growing along the transparent tube are accessible to cameras. Additionally, the variety and complexity of field situations can significantly impact root system architecture (Lynch 1995; Clark *et al.* 2011) and makes the elucidation of the genetic and developmental basis of root system architecture particularly challenging. Combinations of field-, greenhouse-, and laboratory-based approaches are needed to address these questions. In lab conditions, plants can be subjected to controlled combinations of various abiotic and biotic stress factors simultaneously simulating environmental scenarios to which plants are exposed under natural conditions. Such approaches facilitate the identification of genetic components responsible for certain phenotypes or yield increases which may play as well a key role under field conditions. Typically, insight into root systems can be extrapolated from plants grown in artificial substrates, including transparent agarose gel or gellan gum (Nagel *et al.* 2006; Iyer-Pascuzzi *et al.* 2010), paper rolls (Zhu and Lynch 2004), growth pouches consisting of blotting paper covered by plastic foil (Hund *et al.* 2009), and hydroponic cultures (Jones 1982; Tuberosa *et al.* 2002). These cultivation procedures combined with appropriate imaging setups allow optical visualisation and quantification of entire root system architecture in 2D (Walter *et al.* 2002; Armengaud *et al.* 2009; Hargreaves *et al.* 2009; Nagel *et al.* 2009) or reconstructions in 3D if images from numerous camera view angles are acquired (Iyer-Pascuzzi *et al.* 2010; Clark *et al.* 2011). However, these methodologies have several drawbacks, such as absence of microbial interactions, soil structure and, in most cases, even absence of mechanical impedance. In addition, it remains difficult to create heterogeneity of water and nutrient availability typically observed along soil profiles (Hutchings and John 2004). To address these limitations, several labs have experimented with techniques to obtain information about root structure and function from plants grown in natural substrates, such as transparent soil-filled columns or rhizotrons (Thaler and Pagès 1995; Giuliani *et al.* 2005; Watt *et al.* 2006). The observation of roots at transparent interfaces is one of the earliest non-destructive techniques for studying root growth in soil and was first introduced in the 19th century (Sachs 1873). Shape and volumes of rhizotrons vary depending on the research objective and range from small boxes designed to study *Arabidopsis* roots in the lab (Devienne-Barret *et al.* 2006) to large containers, underground cellars, or walkways enclosing natural soil profiles under field conditions for direct observations of tree roots (Hilton *et al.*

1969; Taylor *et al.* 1990). The indisputable advantage of rhizotrons is the opportunity to perform repeated measurements of the same roots at frequent time intervals. When the thickness of rhizotrons is limited to less than 10 mm and a translucent substrate is used, 2D light transmission images can be used to explore the dynamics of root water uptake of the root system (Garrigues *et al.* 2006). For opaque substrates, recently developed techniques like x-ray computed tomography (CT; Heeraman *et al.* 1997; Gregory *et al.* 2003; Pierret *et al.* 2003; Hargreaves *et al.* 2009; Tracy *et al.* 2010; Moradi *et al.* 2011) and nuclear magnetic resonance imaging (MRI; Menzel *et al.* 2007; Jahnke *et al.* 2009; Nagel *et al.* 2009) have made considerable progress. Both techniques facilitate the non-destructive investigations of 3D geometry of root systems grown in soil, but are not yet appropriate to phenotype root systems at a high-throughput (e.g., hundreds of plants per day). Additionally, frequent measurements of the same root system using CT should be avoided, due to the risk of unpredictable effects of high-energy radiation on plant growth. In summary, CT and MRI play an essential role in elucidating the mechanistic understanding of root structure and function, but for screening relatively large plant populations at high frequency and high throughput traditional optical sensors are more appropriate using scanner- or camera-based image acquisition systems. Robotised equipment for imaging plants greatly facilitates high-throughput phenotyping, maximising speed and permitting standardisation. For screening shoots of monocot or dicot plants several techniques have been implemented (Granier *et al.* 2006; Jansen *et al.* 2009; Rajendran *et al.* 2009), however, automated systems for phenotyping root system architecture of plants grown in transparent soil-filled containers are lacking so far.

To start addressing these needs, the aim of this study was to design and deploy a prototype for automatically analysing root system architecture in 2D for plants grown in rhizotrons. The novel setup, GROWSCREEN-Rhizo, allows simultaneous imaging of root and shoot growth of 60 rhizotrons per hour (total capacity of the setup are 72 rhizotrons). For validation two dicot (*Arabidopsis* and rapeseed) and four monocot (*Brachypodium*, barley, rice and maize) plant species were analysed with this setup and the hypothesis was tested whether the part of the root system visible at the transparent face of the rhizotrons is representative of the total root system. Furthermore, we investigated whether the correlation between the visible and hidden part of the root systems is depended on the root diameter of different species or on environmental conditions. In addition, we show the potential of the novel system by investigating the reaction of root growth dynamic and root system development of barley and maize plants to different soil compaction levels.

Materials and methods

Plant material, experiments, and soil cultivation protocols

To validate the novel system, we compared the vertical distribution of monocotyledonous and dicotyledonous root systems within rhizotrons (experiment 1) and quantified the projected shoot area of monocotyledonous plants by analysing images taken from different camera angles (experiment 2). In addition, we tested the correlation of visible root length with total root system length and plant development (experiment 3) and the potential of the system was shown by analysing the effect of soil compaction on shoot and root growth and root system architecture (experiment 4).

In experiment (1), the following plant species were analysed: *Arabidopsis thaliana* (L. Heynh.) ecotype Col-0, *Brachypodium distachyon* (L.) P. Beauv. (GRA 788, Genebank Gatersleben, Germany), *Brassica napus* (L.) cv. Campino (rapeseed), and *Hordeum* vulgare (L.) cv. Barke (barley). In experiment (3) the same plant species were examined and additional *Oryza sativa* (L.) cv. Dom Sufid (rice, IRGC 117265, International rice research institute, Metro Manila, Philippines) and *Zea mays* (L.) cv. Badischer Gelber (maize). While seeds of *Arabidopsis*, *Brachypodium*, rapeseed, and rice were sown in small rhizotrons (60 x 30 x 2 cm), barley and maize were grown in larger rhizotrons (90 x 60 x 3.4 cm). The rhizotrons, consisting of black or light grey polyethylene and one transparent polycarbonate plate, were filled with black peat soil (Graberde; Plantaflor Humus, Vechta Germany; containing N, approx. 120 mg l^{-1}; P_2O_5, approx. 20 mg l^{-1}; K_2O, approx. 170 mg l^{-1}). For correlation of projected leaf area with shoot biomass (experiment 2) *Zea mays* (L.) cv. Helix and *Hordeum vulgare* (L.) cv. Barke were cultivated in peat soil 'ED73' (Einheitserde, Balster Einheitserdewerk, Fröndenberg, Germany; N, approx. 250 mg l^{-1}, P_2O_5, approx. 300 mg l^{-1}, K_2O, approx. 400 mg l^{-1}). In addition, to test the effect of soil compaction on root growth (experiment 4), *Zea mays* (L.) cv. Badischer Gelber was sown in silty clay loam soil collected from a field site at the Klein-Altendorf agricultural station (University of Bonn) in Germany. Four days old seedlings of *Hordeum vulgare* cv. Golden promise germinated on filter paper were transplanted in rhizotrons with different compacted black peat (Reiner Hochmoortorf; Florabella Tuintorf, Geeste, Germany; N, approx. 35 mg l^{-1}; P_2O_5, approx. 30 mg l^{-1}; K_2O, approx. 40 mg l^{-1}) mixed with basalt grit (1:2.3 w/w). Fine powdered gardening lime (95% $CaCO_3$, trace elements) was mixed with the peat (1:50) to adjust the pH of the substrate to 6.5.

To standardise compaction protocols across replicate rhizotrons, portions of 500 g or 1000 g substrate were poured gradually and compressed as described below. The substrate was compacted using a custom-built compaction frame including a manual pallet fork-lift for lifting individual rhizotrons while applying a defined pressure to the soil surface by means of a wooden plank. Applied pressure and compaction values were calculated using a scale. Two draining drills with a diameter of 0.8 cm at the bottom of the rhizotrons, together with a layer of hygroscopic foam (10 cm, Mosy GmbH, Thedinghausen, Germany) maintained sufficient drainage and oxygen supply to the roots (approx. 20% by volume, data not shown).

All plants were supplied with tap water (approx. 7 mg l^{-1} N, 0.5 mg l^{-1} P, 2.6 mg l^{-1} K, 14 mg l^{-1} Mg; 440 µS cm^{-1}), except for rice and barley plants grown in the peat/basalt grid mix, which were supplied with nutrient solution (rice: 7.1 mmol l^{-1} N, 0.52 mmol l^{-1} P_2O_5, 2.05 mmol l^{-1} K_2O, 320 µmol l^{-1} Mg, 7.45 µmol l^{-1} Si, 1.1 µmol l^{-1} Fe and barley: 24.9 mmol l^{-1} N, 1.3 mmol l^{-1} P, 1.75 mmol l^{-1} K, 27.9 nmol l^{-1} Si). To keep a soil water content of approx. 30% (VWC), plants were watered regularly, while the frequency and amount of water or nutrient solution depended on the size of the rhizotrons (small rhizotrons: three times per week 60 ml; large rhizotrons: two times per day 400 ml). Plants were grown in the PhyTec greenhouse of the Institute Plant Sciences (IBG-2; Forschungszentrum Jülich GmbH, Jülich, Germany), which is covered by a specially formulated micro-structured glass (Centrosolar Glas, Fürth, Germany) with high transparency for photosynthetically active radiation (PAR) and ultraviolet (UV) radiation (up to 97% in visible light and up to 35% UV-B transmittance). Environmental conditions were: day length of 16 h, day / night temperatures of approx. 24°C / 18°C and supplemental illumination (SON-T AGRO 400, Philips) was automatically turned on when the ambient light intensity outside the greenhouse was < 400 µmol m^{-2} s^{-1} between 6 a.m. and 10 p.m.

Automated phenotyping of root system architecture and shoot growth

We designed the GROWSCREEN-Rhizo setup (Fig. 1) in collaboration with the company Maschinenbau Kitz GmbH (Troisdorf, Germany) who built the prototype and provided automation control. The rhizotrons were custom-built at Forschungszentrum Jülich GmbH and the final automation protocols and imaging setup were realised at our institute. The imaging platform enables measuring simultaneously development of leaf area and root systems for plants grown in up to 60 rhizotrons per hour. Plants can be analysed with this setup until shoot reaches a height of max. 80 cm or roots reach the bottom of the rhizotrons (max. depth 90 cm). Consequently, the duration of experiments is restricted to a certain time

period after germination corresponding, for example, to four weeks for maize plants or up to flowering time point for *Arabidopsis* plants in our conditions.
The prototype is located in the PhyTec greenhouse facility and consists of two rows of mounting frames in which rhizotrons (outer dimensions: 90 x 70 x 5 cm) are inserted. However, individual or multiple smaller rhizotrons can be inserted by using adapters. The rhizotrons consist of one transparent polycarbonate plate. To prevent light from reaching roots and also algal growth in the soil, the transparent side of the rhizotrons is shielded by an opaque plate combined with dense, black brush curtains (Fig. 1). The inclination angle of the rhizotrons can be adjusted from 0° (vertical) to 43° with the transparent plate of the rhizotrons facing downwards. Rhizotrons are placed in two rows; each row is split into two groups which can be treated separately (Fig. 1). In total, 72 positions exist in which rhizotrons or adapters for one or more rhizotrons can be inserted and each position has a unique ID. Between both rows of rhizotrons a cabinet for imaging rhizotrons is moved automatically on a linear axis with a bi-directional motion. Users can define in which order the cabinet will reach rhizotrons for analysis. To draw a rhizotron into the imaging cabinet, the analysis sleds carrying cameras and light panels inside the cabinet are adapted to the angle of the compartment the rhizotron is being drawn from. This ensures that rhizotrons are kept at the same angle during both cultivation and imaging. A change of the inclination angle would lead to a modified gravitropic signal. After adjusting the angle, the rhizotron is positioned inside the imaging cabinet by a mechanical swivel arm pulling each rhizotron at a hook mounted on one side. The motion into the cabinet is facilitated by slide bars and roller bearings. The motor drawing the rhizotrons is able to actuate completely sand-filled rhizotrons (up to 80 kg). Subsequently, the doors of the cabinet are closed with rolling cutter gates to prevent light conditions influencing image acquisition. Inside the cabinet, two side-view images of the shoot were acquired by two cameras (5 MP camera, GRAS-50S5C, Point Grey Research Inc, Vancouver, Canada; combined with 8 mm FL compact fixed focal length lens, NT56-526, Edmund Optics GmbH, Karlsruhe, Germany) mounted at an angle of 90° to each other and one image of the whole transparent rhizotron surface is acquired with a high resolution camera (16 MP camera, IPX-16M3-VMFB, Imperx, Inc, Boca Raton, Fl, USA; combined with Zeiss Distagon T 2,0/28 ZF-I lens, Jena, Germany). The resolution of the acquired images (230 µm per pixel) is high enough to detect the roots of the evaluated plant species. Illumination is provided by using LED-panels (LED Light Source SL3500-W-J, cool white, colour temperature 8000 K, Brno, Czech Republic) which are turned on synchronized with image acquisition. This temporary illumination pattern, equal to all plants, did not show any

significant effect on root growth which could be revealed by comparing undisturbed and regularly screened plants (not shown). The light panels' position and angle were adjusted to prevent reflections in the images. To increase the contrast between plant and background and to avoid reflections, the cabinet is equipped with black walls. After image acquisition the gates are opened and the rhizotron is placed back to its initial position completing the routine. These steps are repeated automatically for each user-defined position. The whole procedure is automated and driven by a custom software program implemented with LabVIEW®.

For automatic irrigation of plants, a system (T1030plus, Gardena Deutschland GmbH, Ulm, Germany) was installed equipped with four drippers per rhizotron (Fig. 1). The drippers are uniformly distributed over the length of the rhizotrons and allow irrigation of the plants at a user-defined frequency and volume (+/- 2%). Each rhizotron contains two drainage holes to release gravimetrically the excess irrigation solution, which is released into a canalisation system mounted below the rhizotrons and can be collected for physical-chemical analyses. Sensors can be installed inside the rhizotrons to monitor, for example, soil moisture content, soil temperature, or pH and oxygen with planar optodes (Blossfeld *et al.* 2011), respectively.

Analysis of root system architecture

Images and image sequences of root systems acquired with GROWSCREEN-Rhizo were analysed by using the software GROWSCREEN-Root as described, with modifications (Mühlich *et al.* 2008; Nagel *et al.* 2009). We originally developed this software to quantify root growth and root system architecture of plants grown in agar-filled Petri dishes. While in agar-grown plants whole root systems are visible and automatic tracking and extraction of root traits can be done routinely (Nagel *et al.* 2009), only the portion of the root system growing along the transparent plate of rhizotrons is accessible to imaging (Fig. 2). Some roots grow temporarily or permanently within the soil substrate. Consequently, it is not possible to extract a complete tree model for the whole root systems of rhizotron-grown plants, which is the requirement of the software GROWSCREEN-Root (for details see Mühlich *et al.* 2008; Nagel *et al.* 2009). As a result, we adapted the software to allow manual tracking of those roots which could not be detected automatically. Manually tracing roots can be quite time consuming. Using computer mouse graphics tablet with pens (Wacom Cintiq 21UX, CANCOM Deutschland GmbH, Düsseldorf, Germany) to trace individual roots can speed up the image analysis. Additionally, we implemented a batch analysis routine to overlay root structures of subsequent images for any given time series. This feature further reduces time for analysing images by tracing only newly developed roots. The time required for image analysis depends on the complexity of root systems and the frequency of image acquisition, and varies between minutes to hours. We conclude that, to reach the goal of matching the same throughput in image acquisition and processing especially for complex root systems and low contrast backgrounds the software will need to be further improved in the future. The structure of all roots - manually or automatically detected – is then integrated, depicted in a false-colour image (Fig. 2 b, d) and used to determine the following root parameters: root length, branching rates and angles, and spatial distribution of roots within the substrate. Root traits can be divided into global ones – derived from the entire visible part of the root system - and local ones – derived from individual roots. Global traits include total length of all visible roots, root length density (root length per surface area of rhizotrons) quantified at certain substrate layers, rooting depth representing the maximal vertical depth of a root system, and root system width representing the maximal horizontal width of a root system. Traits resulting from performance of individual roots comprise length and number of roots including different root orders, such as main roots (including shoot borne roots) and lateral roots (Fig. 2) branched from main roots as well as angles of roots. Branching angles of lateral roots represent the angle between a main and a branched lateral root and emerging angles of main roots represent the angle between horizontal and main roots. The novel device GROWSCREEN-Rhizo enables the measurement of the same individuals repeatedly in a user-defined frequency (hours or days, respectively). Consequently, all root traits can be quantified at a single time point or related to dynamic changes in characteristics of root system architecture.

To correlate visible roots (from 2D imaging) with total root length and biomass, roots were carefully washed out of the soil and scanned (600 dpi, flatbed scanner, Canon Scan LIDE 60, Canon, Krefeld, Germany). Total root system length was then determined either by tracing roots with GROWSCREEN-Root or with a commercial software (WinRHIZO 2012, Regent Instruments; settings: grey value threshold 30; removal of objects with an area < 1 cm² and a length-width-ratio < 4). Dry weight of both roots and shoots were determined after samples had been oven-dried at 70°C for about 48 h or until constant weight was reached.

Analysis of shoot growth and estimation of shoot biomass

For monocotyledonous plants, like maize and barley, colour images from two side-views at a 90° horizontal rotation were used to quantify the projected leaf area. The amount of pixels corresponding to projected leaf area was determined automatically with custom-made algorithms that allowed segmentation for thresholds of the parameters hue, saturation and value and therefore distinguishing between plant and background (Walter *et al.* 2007). To compare the projected leaf area quantified from images with real leaf area, leaves of each maize and barley plant were scanned (300 dpi, flatbed scanner, Canon Scan LIDE 60, Canon, Krefeld, Germany). For these purposes, plants were harvested at different developmental stages up to 6 weeks after sowing. At each time point, ten maize and barley plants were harvested and fresh weight of shoot was measured to correlate shoot biomass with detected leaf area.

Statistical analysis

The effect of mechanical impedance on root growth and spatial distribution of roots within rhizotrons were analysed using student's t-test (SigmaStat, Systat Software Inc., Richmond, CA, USA).

Results

GROWSCREEN-Rhizo enables quantification of root and shoot growth non-invasively

To evaluate the precision of the software tool for analysing growth and geometry of visible parts of root systems growing along the transparent plate of rhizotrons, reference objects with defined lengths were inserted in rhizotrons. The strong linear correlation ($R^2 = 0.999$) between the real length and the length of those objects quantified with the software GROWSCREEN-Root point out the high precision of the novel image-based tool and its value for root phenotyping (Fig. 3). Based on this, we could, for instance, analyse the vertical distribution within rhizotrons of both monocotyledonous and dicotyledonous root systems (Fig. 4, experiment 1). Generally, dicots exhibited a higher root length density in the upper than in the deeper soil layers. The dicot model plant *Arabidopsis* exhibited a root length density of up to 0.9 cm cm^{-2} surface area of rhizotrons in the top 15 cm, which strongly decreases in deeper substrate layers (Fig. 4 a). In rapeseed, a similar result was found with a root length density of up to 0.8 cm cm^{-2} in the upper 15 cm of rhizotrons (Fig. 4 b). Nevertheless, at a comparable root system length of approx. 260 cm, root system of rapeseed plants reached deeper substrate layers compared with *Arabidopsis* (55 vs. 30 cm, respectively). Consequently, root length density of rapeseed plants declined less sharply in deeper zones of the rhizotrons. In contrast to dicots, *Brachypodium* and barley produced fewer roots in the upper soil layers. Both plants exhibited the maximal root length density already in the top 5 cm, however, with lower average values: 0.7 cm cm^{-2} (*Brachypodium*) and 0.5 cm cm^{-2} (barley), respectively. On the basis of this contrasting behavior in the top soil together with a more gradual decrease of root length density in deeper substrate layers of monocot compared with dicot species, the spatial distribution of monocots and dicots varied significantly ($P \leq 0.05$ at depth of 10-13 cm and 26-36 cm (model species; Fig. 4 a); $P<0.05$ at depth of 6-13 cm and 33-46 cm (crop species; Fig. 4 b)). These observations indicate that this method facilitates the quantitative evaluation of the spatial distribution of roots within the soil profile, which represents a valuable root trait connected to water and nutrient accessibility.

To calculate projected leaf area during shoot development of monocotyledons we used images taken from two side-views at a 90° horizontal rotation angle. To evaluate the precision of the analysis, the image-based method was calibrated against destructive measurements of total leaf area and shoot biomass (experiment 2). When the sum of projected leaf area of both 2D images was compared with leaf area quantified by scanning leaves, we found that linear regression captures the variation (Fig. 5 a, b). The leaf area determined from the sum of projected leaf area from both images seem to slightly overestimate total leaf area of maize (about 2%) and even more for barley plants (about 12%) due to more complex shoot architecture of the latter. Despite this overestimation the correlation coefficient for 100 barley plants at different developmental stages (up to six weeks after sowing) was $R^2 = 0.97$ (Fig. 5 a) and for 80 maize plants even larger $R^2 = 0.99$ (Fig. 5 b). Similar linear correlations were found when the projected leaf area estimated from the two side-view images was plotted against the shoot biomass ($R^2 = 0.95$ for barley (Fig. 5 c); $R^2 = 0.98$ for maize plants (Fig. 5 d)). This result implies that leaf area quantified non-invasively by images taken from two side-views at a 90° horizontal rotation can be sufficient to estimate shoot development at early vegetative stages.

The visible portion of the root system in rhizotrons is correlated with the total length of the root system for different species

Our novel screening device was specifically designed to enable standardised routine evaluation of growth and architecture of roots grown in soil-filled rhizotrons non-invasively. However, a disadvantage of rhizotrons is that only a part of the root system is visible at the transparent plate of the containers. The proportion of roots reaching the transparent plate that is accessible for image analysis is dependent on the inclination of the rhizotrons with respect to the ground (experiment 3). Generally, the more the rhizotron is inclined (with the transparent side of rhizotrons facing downwards), the higher the proportion of visible roots compared to the entire root system. While only approx. 14% of the total root system of barley plants grown in vertical rhizotrons (inclination angle of 0°, representing the angle between the vertical line and the rhizotrons) was visible, this percentage increased to approx. 24% at an inclination angle of 25° and was approx. 33% at an inclination angle of 43° (representing the maximum inclination angle of the GROWSCREEN-Rhizo setup), respectively (data not shown). Additional to the inclination angle of rhizotrons, we tested if soil properties, in particular mechanical impedance affect the fraction of visible roots. While a moderate increase in soil compaction by 2-3 times (up to 0.16 MPa (maize) and 0.78 MPa (barley)) compared with low compacted soil resulted in specific root weight increases for both barley (+38%) and maize plants (+11%), the fraction of visible roots was only marginally reduced for barley plants (-2%) and slightly increased for maize plants (+4%, Tab. 1). In contrast to the inclination angle of rhizotrons, we observed that moderate soil mechanical impedance on developing roots had a negligible effect on the proportion of roots which are visible at the transparent plate of rhizotrons.

For further confirmation of the correlation between the visible and total root system length, we analysed four monocot and two dicot plant species under comparable growth conditions including inclination angle of rhizotrons of 43° (for more details, see Material and Methods). Linear correlations were found between the root length visible at the transparent surface of soil-filled rhizotrons and the total root system length for all examined plant species (Fig. 6 a). The correlation coefficients ranged from $R^2 = 0.91$ for barley plants up to $R^2 = 0.97$ for rapeseed plants, with the exception of maize ($R^2 = 0.51$). However, the slopes of linear regression curves varied between species: both examined dicot species (*Arabidopsis* and rapeseed) showed curves with steeper gradient compared to the monocot species, rice, barley, *Brachypodium,* and maize, respectively (Fig. 6 a). These results show that the percentage of visible roots compared to total root system differs between plant species in our setup. *Arabidopsis* roots grown in rhizotrons positioned on average 77% of the entire root system along the transparent plate and rapeseed plants approx. 42%. In the examined monocot species comparatively less roots are visible; 33% barley, 32% rice, 24% *Brachypodium*, and only 17% of maize root system are accessible (Fig. 6 a, Tab. 2). To some extent, the fraction of roots visible along the transparent plate was related to the specific root weight for the examined plant species. The higher the proportion of visible roots, the lower the specific root weight, which ranged from 0.5 mg m^{-1} in *Arabidopsis* to 24.5 mg m^{-1} root biomass per unit root length in maize plants (Tab. 2). One exception was *Brachypodium* that exhibited a relatively low fraction of visible roots together with a low specific root weight of 1.7 mg m^{-1}.

Additionally, we tested to what extent the visible root length may also be a measure for root biomass. Similar to the correlation of visible root length with total root length, we found that the visible fraction correlated with root dry weight of different plant species (Fig. 6 b). Furthermore, visible root length exhibited linear correlations with development of aboveground plant organs, shoot biomass (Fig. 6 c) as well as leaf area development (Fig. 6 d). Comparable to the results obtained for the correlation between visible and total root system length, the slopes of linear regression curves differed between plant species. *Arabidopsis* plants exhibited the steepest gradient compared to rapeseed, rice, barley, and *Brachypodium* plants; maize showed the weakest gradient (Fig. 6). Accordingly, at a comparable visible root length of 300 cm, maize plants produced 75 times more root biomass, 14 times more shoot biomass, and a 9 times larger leaf area than *Arabidopsis* plants.

Moderate increases in soil strength affect root system architecture of barley plants

As a first application of the novel system GROWSCREEN-Rhizo we devised a protocol to study the reaction of root growth dynamic and root system development in response to varying soil compaction levels in rhizotrons (Fig. 7, experiment 4). Soil compaction is a factor that may significantly limit the development of root systems in the field. To understand the potential of the system, we chose to apply a relatively moderate soil compaction level of 0.52 MPa (moderate compaction) compared with low compaction of 0.06 MPa (low compaction). The outcome of this relatively small increase in soil strength was a comparable leaf area development (Fig. 7 a) with similar shoot growth rates (14.4 +/- 1.3 % d^{-1} (low) vs. 15.5+/-1.2 % d^{-1} (moderate)) as well as similar leaf mass per area values (22.9 +/- 0.6 g m^{-2} (low) vs. 21.9 +/-1.3 g m^{-2} (moderate)) of barley plants grown under both soil compaction levels. In contrast to the shoot, root systems of barley plants responded significantly to these small changes in compaction levels. The increased soil compaction led to 26% shorter main root length compared to plants grown under low compaction (Fig. 7 b; $P<0.05$ day 8-17). At both soil compaction levels, lateral roots emerged eleven days after sowing but already three days later growth of lateral roots was significantly reduced when soil compaction was moderately increased (Fig. 7 c; $P = 0.028$). In total, lateral root systems of plants grown under 0.52 MPa were 34% shorter than those of plants grown under 0.06 MPa. In a similar range rooting depth was inhibited by soil strength. Until the end of observation (day 20) roots did not reach the bottom of the rhizotrons. Soil compaction affected not only the root growth rate, but also the spatial distribution of roots within the rhizotrons (Fig. 7 d). The soil was homogeneously compacted within the rhizotrons, except for the top 5 cm, which were filled in both conditions

- low and moderate compaction – with loose soil. Interestingly, plants grown in more compacted soil, induced significantly root growth into this top soil layer (P = 0.004). However, below a depth of approx. 25 cm, root length density of plants grown in moderate compacted rhizotrons revealed a strong decrease. This reduction was significant in the horizon starting at 32 cm and including deeper soil layers (Fig. 7 d; P = 0.039). In conclusion, these results highlight that the automated rhizotron cultivation system and the imaging routine enable detection of changes in root length and geometry of root systems caused by relatively moderate mechanical stresses.

Discussion

The novel method GROWSCREEN-Rhizo enables to phenotype root systems and correlate root traits to whole plant development

The novel phenotyping system presented here, which we named GROWSCREEN-Rhizo, is capable to deliver quantitative information on root system development and plant performance of rhizotron-grown plants. These are essential information to tackle biological questions stemming from both basic research as well as from breeding processes. For example, this method is applicable to detect differences in root system architecture induced by relatively moderate increases in soil compaction (Fig. 7). An increase in soil compaction from 0.06 to 0.52 MPa resulted in significant reduction in growth of main as well as lateral roots of barley plants (Fig. 7 b, c). It has been reported for several species that root elongation rate varies inversely with soil resistance within a range of 0 to 7.5 MPa (e.g., Atwell 1993; Bengough *et al.* 2011). In our experiments mechanical impedance due to compaction of the soil caused not only a reduction of root growth but also of the spatial distribution of roots along the soil profile. An increase in soil strength resulted in a shift of root distribution to the top soil layers while rooting depth was decreased (Fig. 7 d). These results obtained in soil-filled rhizotrons are in line with findings obtained in the field (Lipiec *et al.* 1991). While root system development was reduced under moderate soil compaction in our rhizotrons, leaf growth was unaffected (Fig 7 a). This is apparently in contrast to the findings of Beemster *et al.* (1996) who showed that resistance to root penetration leads to a reduction in leaf cell elongation of wheat plants, while leaf growth is more strongly affected compared with root growth (Masle 1992). The discrepancy between these studies and our findings can be explained by the much higher level of soil compaction (7.5 MPa) which Beemster *et al.* (1996) applied compared with the treatments in our experiments. Apparently, a certain threshold of soil resistance to root penetration has to be reached to affect leaf growth. This hypothesis is confirmed by Lipiec *et al*. (1991) who showed that high levels of soil resistance are needed to decrease leaf area index of barley plants grown in the field. However, the degree to which the reduction in root development triggered by mechanical impedance reduces shoot biomass or yield also depends on the extent of restriction in water and nutrient uptake (Clark *et al.* 2003).

The distribution of root length per unit volume in the soil profile is the key to extract sufficient water and nutrients (Gregory *et al.* 2009). Differences in root length density along the depth of rhizotrons were also detected when monocot and dicot species were screened (Fig. 4). While the dicot species *Arabidopsis* and rapeseed exhibited a higher root length density in top substrate layers, lower values were found in deeper layers compared with the monocot species, *Brachypodium* and barley. These modifications can be ascribed to morphological differences of monocot and dicot root system. The allorhizic root system of dicotyledons is characterised by the development of one primary root and lateral roots which start branching at the base of the root system (Osmont *et al.* 2007). Consequently, during the first weeks after germination, a higher root length density would be expected in top soil layers. Yet, in homorhizic root systems such as those of monocots, many adventitious roots develop in parallel to the primary root (Osmont *et al.* 2007) and lead to a higher root length density in deeper layers.

In addition to non-invasive phenotyping of root systems GROWSCREEN-Rhizo offers the advantage to screen root and shoot growth simultaneously and correlate root traits to whole plant development. The non-destructive analysis enables to compare the impact of treatments at various reference stages, e.g., at the same leaf area size. Therefore, it is possible to distinguish if a treatment affects the speed of development or if it has direct interactions with plant development. For dicotyledonous plants, like *Arabidopsis* or tobacco seedlings that have leaves which spread out almost horizontally at midday, projected leaf area development can be quantified automatically by acquiring images of leaves from the top view of the plants (Granier *et al.* 2005; Walter *et al.* 2007). Leaf growth of monocots, such as barley and maize can be estimated by images taken from different camera angles. We show that the projected leaf area correlated linearly with the shoot biomass of barley and maize plants ($R^2 > 0.95$; Fig. 5). Similar correlations were found previously by using a commercially available plant image capture and analysis system (Rajendran *et al.* 2009). Since these methods resulted in similar correlation coefficients ($R^2 = 0.94$ for wheat (Rajendran *et al.* 2009), $R^2 = 0.95$ for barley (Fig. 5 c) and $R^2 = 0.98$ for maize (Fig. 5 d), respectively), our imaging setup appears to be sufficient to estimate plant biomass as a linear function of the projected leaf area for the examined monocot species at early vegetative stages characterised by moderate overlap of different leaves. For further improvement the accuracy of biomass estimation, Golzarian *et al.* 2011 presented a model for wheat and barley plants which integrates information obtained from the images with plant age. However, using projected shoot area as an estimator of shoot biomass requires validation for different species characterised by diverse shoot architecture and depending on different treatments simulating environmental scenarios.

The fraction of visible part of the root system in rhizotrons is correlated with the total root system and plant development

Growing plants in rhizotrons facilitates non-invasive measurements of the same individual at frequent time intervals. However, even if roots are forced to grow towards the transparent plate by inclining rhizotrons, only a part of the root systems is visible and accessible for cameras (Fig. 6 a, Tabs. 1, 2). The proportion of visible roots at the transparent interface of rhizotrons depends slightly on soil strength (Tab. 1) and can be enhanced by increasing the inclination angle of rhizotrons (with the transparent side facing downwards). Consequently, to standardise protocols and achieve reliable comparisons between individual plants, it is necessary not only to ensure homogeneous filling of the rhizotrons but also control their inclination angles. In addition, the percentage of visible roots varies between plant species (Fig. 6 a, Tab. 2). The fraction of visible roots seems to be related to specific root weight and root diameter of plant species: the thinner the roots, the higher the percentage of visible roots: While a relatively large proportion of thin roots of *Arabidopsis* plants (root diameter approx. 100µm; Van der Weele *et al.* 2000) was visible (approx. 77%), the smallest fraction of roots was visible (about 17%, Tab. 2) when roughly ten times thicker roots of maize plants (Van der Weele *et al.* 2000) were observed in rhizotrons. Rapeseed, barley, rice, and *Brachypodium* plants exhibited values ranging between those of *Arabidopsis* and maize plants (Tab. 2; e.g., Hargreaves *et al.* 2009; Watt *et al.* 2009). Kuchenbuch and Ingram (2002) reported similar results for maize (about 20%) and Hurd (1963) showed for wheat plants that the visible root length represents approx. 30% of total root system length. Consequently, the visible part of the root system can only be used as a measure for growth of total root system if differences between species are taken into consideration and well-defined protocols are used. In addition, the assumption that the visible part is a constant fraction of the total root system must always be thoroughly checked before analysing new species or changing environmental conditions such as soil structure, soil water content, or root zone temperature. Beside the correlation between the visible and the total root system, it is useful to address if root and shoot growth profiles observed in rhizotrons are comparable with those detected in other growth media and conditions. Further studies are needed to test if the transparent plate of rhizotrons - along which roots are forced to grow - modifies root growth and / or root system architecture and if the root traits observed in rhizotrons are relevant under field situations. For this approach not only field but also agar-grown plants can be taken into account due to the visibility and accessibility of whole root systems in transparent media. The combination of different methods and approaches under artificial and natural environments and the integration at different scales into "phenotyping chains" will improve our knowledge of the hidden half of plants and will open novel routes for plant breeding (De Smet *et al.* 2012).

Simple root morphological traits have higher heritability values compared with global architectural traits

The novel system GROWSCREEN-Rhizo enables the measurement of simple morphological traits (e.g., root length) and global architectural traits (e.g., width and depth of root system and root length density profiles) of root systems of different species (Figs. 5-8, Tab. 3). The possibility to quantify branching angles of lateral roots or angles in which main and shoot borne roots emerge in rhizotrons depends on the visibility of the branching/starting point of roots. Due to the fact that often parts of individual roots are hidden in the soil, the quantification of the number of main, shoot borne or lateral roots is challenging in rhizotron-grown plants. Since root system architecture is not well explored to date, it may be worth to measure as many root traits as possible. Scaling the novel system to a desired throughput and improving further the software for automated analyses of root systems will enable phenotyping of large numbers of genetic diverse genotypes. This is indispensable to evaluate the relevance of measured roots traits and to find heritably traits correlated with resource use efficiency, performance and yield of plants. Especially, for breeding strategies heritable traits play a key role. In contrast to root biomass, which appears to have low heritability values (Jones 1977), moderate and high heritability values were reported for root length of main and lateral roots as well as for total root systems (Tab. 3). Highest heritability values were found for root length of potato and cotton plants with h^2 of up to 0.99 (Anithakumari *et al.* 2011; Malik *et al.* 2011). Heritability was in general slightly lower under drought or salt stress than under control conditions (e.g., Dhanda *et al.* 2004; Anithakumari *et al.* 2011; Arraouadi *et al.* 2011). In the presence of Zn concentration ranging from 1 to 250 µM the broad sense heritability varies between 0.44 to 0.75 for primary and lateral root length of *Arabidopsis* accessions (Richard *et al.* 2011). Moderate heritability was found for nodal root angle (0.47; Singh et al. 2011), depth of root system (up to 0.53; Ao *et al.* 2010), and only slightly higher heritability values for width of root system (0.62; Ao *et al.* 2010). Based on these studies, root morphological traits have higher heritability values than global architectural ones and could be more valuable for breeding progress. For example, it could be difficult to breed for root length density because of the lowest heritability values and the largest range of variation across seasons and rooting depth (h^2 = 0.14-0.57) compared to other root traits (Kashiwagi *et al.* 2005). However, this literature survey highlights that, to date, heritability values of root system architecture have been published only for a few plant species; as a consequence, caution is necessary in making widely applicable generalizations. Further studies are required and these will accelerate the progress in prediction of genotypic and phenotypic effects during the selection of plant material (Johnson *et al.* 1955; Malik *et al.* 2011). Promising belowground features which should be addressed in breeding programs to improved water and nutrient uptake of plants are for example root growth, branching rate, and root angle (Hammer *et al.* 2009; Herder *et al.* 2010,; Lynch 2011). Optimising these root traits could lead to an increased yield production provided that the right balance in resource allocation between root and shoot is ensured (Lynch 2007).

Conclusion

The novel platform described in this paper is a unique automated prototype to phenotype root system architecture of a diverse set of plant species grown in soil-filled rhizotrons. The system demonstrates a step towards bridging the gap between lab and field and enables to quantify static and dynamic characteristics of root systems, and to correlate them to whole plant growth and development. The evaluation of root traits of a diverse set of genetic resources under a range of environmental conditions will give the opportunity to discover the genetic control of root system architecture. The prototype scaled to a desired throughput (thousands of plants) will represent a valuable tool to characterise gene function and assist breeding pipelines by selecting genotypes with improved plant growth performance, biomass, and yield production.

Acknowledgements

We are indebted to Thorsten Brehm, Marcel Schneider, Beate Uhlig, and Franz-Wilhelm Genzer for installing drainage and irrigation system of the GROWSCREEN-Rhizo setup. We are grateful to Saaten-Union Biotec GmbH for providing us with seeds of *Hordeum vulgare* cv. Golden promise. We thank Birgit Bleise, Anne Dreißen, and Nadja Vöpel for technical assistance during harvest of rhizotron-grown plants.

References

Anithakumari AM, Dolstra O, Vosman B, Visser RGF, van der Linden CG (2011) In vitro screening and QTL analysis for drought tolerance in diploid potato. *Euphytica* **181**, 357-369.

Ao J, Fu J, Tian J, Yan X, Liao H (2010) Genetic variability for root morph-architecture traits and root growth dynamics as related to phosphorus efficiency in soybean. *Functional Plant Biology* **37**, 304-312.

Armengaud P, Zambaux K, Hills A, Sulpice R, Pattison RJ, Blatt MR, Amtmann A (2009) EZ-Rhizo: integrated software for the fast and accurate measurement of root system architecture. *The Plant Journal* **57**, 945-956.

Arraouadi S, Chardon F, Huguet T, Aouani ME Badri M (2011) QTLs mapping of morphological traits related to salt tolerance in Medicago truncatula. *Acta Physiologiae Plantarum* **33**, 917-926.

Atwell BJ (1993) Response of roots to mechanical impedance. *Environmental and Experimental Botany* **33**, 27-40.

Beemster GTS, Masle J, Williamson RE, Farquhar GD (1996) Effects of soil resistance to root penetration on leaf expansion in wheat *(Triticum aestivum* L): kinematic analysis of leaf elongation. *Journal of Experimental Botany* **47**, 1663-1678.

Bengough AG, McKenzie BM, Hallett PD, Valentine TA (2011) Root elongation, water stress, and mechanical impedance: a review of limiting stresses and beneficial root tip traits. *Journal of Experimental Botany* **62**, 59-68.

Blossfeld S, Gansert D, Thiele B, Kuhn AJ, Lösch R (2011) The dynamics of oxygen concentration, pH value, and organic acids in the rhizosphere of Juncus spp. *Soil Biology and Biochemistry* **43**, 1186-1197.

Clark LJ, Whalley WR, Barraclough PB (2003) How do roots penetrate strong soil? *Plant and Soil* **255**, 93-104.

Clark RT, MacCurdy RB, Jung JK, Shaff JE, McCouch SR, Aneshansley DJ, Kochian LV (2011) Three-Dimensional Root Phenotyping with a Novel Imaging and Software Platform. *Plant Physiology* **156**, 455-465.

De Smet I, White PJ, Bengough AG, Dupuy L, Parizot B, Casimiro I, Heidstra R, Laskowski M, Lepetit M, Hochholdinger F, Draye X, Zhang H, Broadley MR, Péret B, Hammond JP, Fukaki H, Mooney S, Lynch JP, Nacry P, Schurr U, Laplaze L, Benfey P, Beeckman T, Bennett M (2012) Analyzing Lateral Root Development: How to Move Forward. *Plant Cell,* DOI 10.1105/tpc.111.094292.

Devienne-Barret F, Richard-Molard C, Chelle M, Maury O, Ney B (2006) Ara-rhizotron: An effective culture system to study simultaneously root and shoot development of *Arabidopsis*. *Plant and Soil* **280**, 253-266.

Dhanda SS, Sethi GS, Behl RK (2004) Indices of Drought Tolerance in Wheat Genotypes at Early Stages of Plant Growth. *Journal of Agronomy and Crop Science* **190**, 6-12.

Garrigues E, Doussan C, Pierret A (2006) Water uptake by plant roots: I – Formation and propagation of a water extraction front in mature root systems as evidenced by 2D light transmission imaging. *Plant and Soil* **283**, 83-98.

Golzarian MR, Frick RA, Rajendran K, Berger B, Roy S, Tester M, Lun DS (2011) Accurate inference of shoot biomass from high-throughput images of cereal plants. *Plant Methods* **7**, 1-11. http://www.plantmethods.com/content/7/1/2.

Gonzalez N, Beemster GTS, Inze D (2009) David and Goliath: what can the tiny weed Arabidopsis teach us to improve biomass production in crops? *Current Opinion in Plant Biology* **12**, 157-164.

Granier C, Aguirrezabal L, Chenu K, Cookson SJ, Dauzat M, *et al*. (2006) PHENOPSIS, an automated platform for reproducible phenotyping of plant responses to soil water deficit in *Arabidopsis thaliana* permitted the identification of an accession with low sensitivity to soil water deficit. *New Phytologist* **169**, 623-635.

Gregory PJ (1979) A periscope method for observation root growth and distribution in field soil. *Journal of Experimental Botany* **30**, 205-214.

Gregory PJ, Hutchison DJ, Read DB, Jenneson PM, Gilboy WB, Morton EJ (2003) Non-invasive imaging of roots with high resolution X-ray micro-tomography. *Plant and Soil* **255**, 351-359.

Gregory PJ, Bengough AG, Grinev D, Schmidt S, Thomas WBTB, Wojciechowski T, Young IM (2009) Root phenomics of crops: opportunities and challenges. *Functional Plant Biology* **36**, 922-929.

Giuliani S, Sanguineti MC, Tuberosa R, Bellotti M, Salvi S, Landi P (2005) *Root-ABA1*, a major constitutive QTL, affects maize root architecture and leaf ABA concentration at different water regimes. *Journal of Experimental Botany* **56**, 3061-3070.

Hammer GL, Dong Z, McLean G, Doherty A, Messina C, Schussler J, Zinselmeier C, Paszkiewicz S, Cooper M (2009) Can changes in canopy and/or root system architecture explain historical maize yield trends in the U.S. Corn Belt? *Crop Science* **49**, 299-312.

Hargreaves CE, Gregory PJ, Bengough AG (2009) Measuring root traits in barley (*Hordeum vulgare* ssp. *vulgare* and ssp. *spontaneum*) seedlings using gel chambers, soil sacs and X-ray microtomography. *Plant Soil* **316**, 285-297.

Heeraman DA, Hopmans JW, Clausnitzer V (1997) Three dimensional imaging of plant roots in situ with X-ray computed tomography. *Plant and Soil* **189**, 167-179.

Herder GD, Isterdael GV, Beeckman T, De Smet I (2010) The roots of a new green revolution. *Trends in Plant Science* **15**, 600-607.

Hilton RJ, Bhar DS, Mason GF (1969) A rhizotron for *in situ* root growth studies. *Canadian Journal of Plant Science* **49**, 101-104.

Hund A, Ruta N, Liedgens M (2009) Rooting depth and water use efficiency of tropical maize inbred lines, differing in drought tolerance. *Plant and Soil* **318,** 311-325.

Hurd EA (1963) Root study of three wheat varieties and their resistance to drought and damage by soil cracking. *Canadian Journal of Plant Science* **44**, 240-248.

Hutchings MJ, John EA (2004) The effects of environmental heterogeneity on root growth and root/shoot partitioning. *Annals of Botany* **94,** 1-8.

Iyer-Pascuzzi AS, Symonova O, Mileyko Y, Hao Y, Belcher H, Harer J, Weitz JS, Benfey PN (2010) Imaging and analysis platform for automated phenotyping and trait ranking of plant root systems. *Plant Physiology* **152**, 1148-1157.

Jahnke S, Menzel MI, van Dusschoten D, Roeb GW, Bühler J, *et al*. (2009) Combined MRI–PET dissects dynamic changes in plant structures and functions. *The Plant Journal* **59**, 634-644.

Jansen M., Gilmer F., Biskup B., Nagel K.A., Rascher U., Fischbach A., Briem S., Dreissen G., Tittmann S., Braun S., De Jaeger I., Metzlaff M., Schurr U., Scharr H., Walter A. (2009) Simultaneous phenotyping of leaf growth and chlorophyll fluorescence via GROWSCREEN FLUORO allows detection of stress tolerance in *Arabidopsis thaliana* and other rosette plants. *Functional Plant Biology* **36**, 902-914.

Johnson N, Robinson HF, Comstock RE (1955). Genotypic and phenotypic correlations in sorghum and simplification in selection. *Agronomy Journal* **47**, 477-482.

Johnson MG, Tingey DT, Phillips DL, Storm MJ (2001) Advancing fine root research with minirhizotrons. *Environmental and Experimental Botany* **45**, 263-289.

Jones A (1977) Heritabilities of Seven Sweet Potato Root Traits. *Journal of American Society for Horticultural Science* **102**, 440-442.

Jones JB (1982) Hydroponics: its history and use in plant nutrition studies. *Journal of Plant Nutrition* **5**, 1003-1030.

Kashiwagi J, Krishnamurthy L, Upadhyaya HD, Krishna H, Chandra S, Vadez V, Serraj R (2005) Genetic variability of drought-avoidance root traits in the mini-core germplasm collection of chickpea (*Cicer arietinum* L.). *Euphytica* **146**, 213-222.

Kuchenbuch RO, Ingram KT (2002) Image analysis for non-destructive and non-invasive quantification of root growth and soil water content in rhizotrons. *Journal of Plant Nutrition and Soil Science* **165**, 573-581.

Laperche A, Devienne-Barret F, Maury O, Le GouisJ, Ney B (2006) A simplified conceptual model of carbon/nitrogen functioning for QTL analysis of winter wheat adaptation to nitrogen deficiency. *Theoretical and Applied Genetics* **113**, 1131-1146.

Lipiec J, Hakansson I, Tarkiewicz S, Kossowski J (1991) Soil physical-properties and growth of spring barley as related to the degree of compactness of two soils. *Soil and Tillage Research* **19,** 307-317.

Lynch J (1995). Root architecture and plant productivity. *Plant Physiology* **109**, 7-13.

Lynch JP (2007) Roots of the second green revolution. *Australian Journal of Botany* **55**, 493-512.

Lynch JP (2011) Root Phenes for Enhanced Soil Exploration and Phosphorus Acquisition: Tools for Future Crops. *Plant Physiology* **156**, 1041-1049.

MacMillan K, Emrich K, Piepho H-P, Mullins C E, Price AH (2006) Assessing the importance of genotype x environment interaction for root traits in rice using a mapping population. I: a soil-filled box screen. *Theoretical and Applied Genetic* **113**, 977-986.

Malik W, Iqbal MZ, Khan AA, Noor E, Qayyum A, Hanif M (2011) Genetic basis of variation for seedling traits in *Gossypium hirsutum* L. *African Journal of Biotechnology* **10**, 1099-1105.

Manschadi AM, Christopher J, deVoil P, Hammer GL (2006) The role of root architectural traits in adaptation of wheat to water-limited environments. *Functional Plant Biology* **33**, 823-837.

Masle J **(**1992) Genetic variation in the effects of root impedance on growth and transpiration rates of wheat and barley. *Australian Journal of Plant Physiology* **19**, 109-125.

Menzel MI, Oros-Peusquens A-M, Pohlmeier A, Shah NJ, Schurr U, Schneider HU (2007) Comparing 1H-NMR imaging and relaxation mapping of German white asparagus from five different cultivation sites. *Journal of Plant Nutrition and Soil Science* **170**, 24-38.

Moradi AB, Carminati A, Vetterlein D, Vontobel P, Lehmann E, Weller U, Hopmanns JW,

Vogel HJ, Oswald SE (2011) Three-dimensional visualization and quantification of water content in the rhizosphere. *New Phytologist* **192**, 653-663.

Mühlich M, Truhn D, Nagel K, Walter A, Scharr H, Aach T (2008) Measuring Plant Root Growth. Pattern Recognition: 30th DAGM Symposium Munich, Germany; *Lecture Notes in Computer Science* **5096**, 497-506.

Nagel KA, Schurr U, Walter A (2006) Dynamics of root growth stimulation in *Nicotiana tabacum* in increasing light intensity. *Plant Cell and Environment* **29**, 1936-1945.

Nagel KA, Kastenholz B, Jahnke S, van Dusschoten D, Aach T, Mühlich M, Truhn D, Scharr H, Terjung S, Walter A, Schurr U (2009) Temperature responses of roots: impact on growth, root system architecture and implications for phenotyping *Functional Plant Biology* **36**, 947-959.

Osmont KS, Sibout R, Hardtke CS (2007) Hidden Branches: Developments in Root System Architecture. *Annual Review in Plant Biology* **58**, 93-113.

Passioura JB (2010) Scaling up: the essence of effective agricultural research. *Functional plant biology* **37**, 585-591.

Pierret A, Kirby M, Moran C (2003) Simultaneous X-ray imaging of plant root growth and water uptake in thin-slab systems. *Plant and Soil* **255**, 361-373.

Rajendran K, Tester M, Roy SJ (2009) Quantifying the three main components of salinity tolerance in cereals. *Plant, Cell and Environment* **32**, 237-249.

Richard O, Pineau C, Loubet S, Chalies C, Vile D, Marquès L, Berthomieu P (2011) Diversity analysis of the response to Zn within the *Arabidopsis thaliana* species revealed a low contribution of Zn translocation to Zn tolerance and a new role for Zn in lateral root development. *Plant, Cell and Environment* **34**, 1065-1078.

Roy R, Mazumder PB, Sharma GD (2009) Proline, catalase and root traits as indices of drought resistance in bold grained rice (*Oryza sativa*) genotypes. *African Journal of Biotechnology* **8**, 6521-6528.

Sachs J (1873). Ueber das Wachsthum der Haupt- und Nebenwurzeln. *Arb. Bot. Inst. Wuerzburg 3,* 395-477, 584-634.

Singh V, van Oosteron EJ, Jordan DR, Hunt CH, Hammer GL (2011) Genetic Variability and Control of Nodal Root Angle in Sorghum. *Crop Science* **51**, 2011-2020.

Taylor HM, Upchurch DR, McMichael BL (1990) Applications and limitations of rhizotrons and minirhizotrons for root studies. *Plant and Soil* **129**, 29-35.

Thaler P, Pagès L (1995) Root apical diameter and root elongation rate of rubber seedlings (*Hevea brasiliensis*) show parallel responses to photoassimilate availability. *Physiologia Plantarum* **91**, 365-371.

Trachsel S, Kaeppler SM, Brown KM, Lynch JP (2011) Shovelomics: high throughput phenotyping of maize (*Zea mays* L.) root architecture in the field. *Plant and Soil* **341**, 75-87.

Tracy SR, Roberts JA, Black CR, McNeill A, Davidson R, Mooney SJ (2010). The X-Factor: visualising undisturbed root architecture in soil using X-ray Computed Tomography. *Journal of Experimental Botany* **61**, 311-313.

Tuberosa R, Sanguineti MC, Landi P, Giuliani MM, Salvi S, Conti S (2002) Identification of QTLs for root characteristics in maize grown in hydroponics and analysis of their overlap with QTLs for grain yield in the field at two water regimes. *Plant Molecular Biology* **48**, 697-712.

Van der Weele CM, Spollen WG, Sharp RE, Baskin TI (2000) Growth of *Arabidopsis thaliana* seedlings under water deficit studied by control of water potential in nutrient-agar media. *Journal of Experimental Botany* **51**, 1555-1562.

Walter A, Spies H, Terjung S, Küsters R, Kirchgeßner N, Schurr U (2002) Spatio-temporal dynamics of expansion growth in roots: automatic quantification of diurnal course and temperature response by digital image sequence processing. *Journal of Experimental Botany* **53**, 689-698.

Walter A, Scharr H, Gilmer F, Zierer R, Nagel KA, Ernst M, Wiese A, Virnich O, Christ MM, Uhlig B, Jünger S, Schurr U (2007) Dynamics of seedling growth acclimation towards altered light conditions can be quantified via GROWSCREEN: a setup and procedure designed for rapid optical phenotyping of different plant species. *New Phytologist* **174**, 447-455.

Watt M, Silk WK, Passioura JB (2006) Rates of root and organism growth, soil conditions, and temporal and spatial development of the rhizosphere. *Annals of Botany* **97**, 839-855.

Watt M, Schneebeli K, Dong P, Wilson IW (2009) The shoot and root growth of Brachypodium and its potential as a model for wheat and other cereal crops. *Functional Plant Biology* **36**, 960-969.

Xing Y, Zhang Q (2010) Genetic and molecular bases of rice yield. *Annual Review of Plant Biology* **61**, 421-442.

Zhu JM, Lynch JP (2004) The contribution of lateral rooting to phosphorus acquisition efficiency in maize (*Zea mays*) seedlings. *Functional Plant Biology* **31**, 949-958.

Tables

Tab. 1: Effect of soil compaction and correlation of visible root length at the transparent surface of rhizotrons with total root length (extracted from fitted linear regression curves for each plant species and growth condition; correlation coefficients (R^2) are given) and specific root weight (mean value +/- SE, n=5-21).

Plant species	Soil compaction level (MPa)	Ratio visible vs. total root length (%)	Root biomass per root length (mg m^{-1})
Hordeum vulgare cv. Golden Promise	0.30	29.4% (R^2 = 0.87)	4.0 +/- 0.5
	0.78	27.2% (R^2 = 0.72)	6.5 +/- 0.6
Zea mays cv. Badischer Gelber	0.07	16.7% (R^2 = 0.51)	24.5 +/- 5.1
	0.16	20.3% (R^2 = 0.94)	27.4 +/- 9.6

Tab. 2: Correlation between visible root length at the transparent surface of rhizotrons with total root length (extracted from fitted linear regression curves of each plant species; correlation coefficients (R^2) are given) and comparison of specific root weight of different plant species (mean value +/- SE, n=11-30). Plants were grown under a soil compaction level of approx. 0.07 MPa and rhizotrons were set to an inclination angle of 43°.

Plant species	**Ratio visible vs. total root length**	**Root biomass per root length (mg m^{-1})**
Arabidopsis thaliana	77% ($R^2 = 0.96$)	0.5 +/- 0.05
Brassica napus	42% ($R^2 = 0.97$)	3.0 +/- 0.6
Hordeum vulgare cv. Barke	33% ($R^2 = 0.91$)	5.5 +/- 0.5
Oryza sativa	32% ($R^2 = 0.95$)	5.5 +/- 0.4
Brachypodium distachyon	24% ($R^2 = 0.93$)	1.7 +/- 0.1
Zea mays cv. Badischer Gelber	17% ($R^2 = 0.51$)	24.5 +/- 5.1

Tab. 3: Root traits measured non-destructively with the novel system GROWSCREEN-Rhizo of plant roots grown in rhizotrons. Broad sense heritability (h^2) values for certain root traits in literature are indicated (n=3-10).

Root traits	**Primary data**	**Plant species**	**Heritability h^2**	**Reference**
Main root length / kinetics	Length of main roots (cm)	*Arabidopsis*	0.44 (1 µM Zn) - 0.75 (250 µM Zn)	Richard et al. 2011
		Wheat	0.42	Laperche et al. 2006
Lateral root length / kinetics	Total length of branched roots (cm)	*Arabidopsis*	0.65 (1 µM Zn) - 0.44 (100 µM Zn)	Richard et al. 2011
		Wheat	0.38	Laperche et al. 2006
Root system length / kinetics	Sum of all visible roots (main, shoot borne and lateral roots) (cm)	Cotton	0.99	Malik et al. 2011
		Potato	0.93 (control) - 0.84 (drought stress)	Anithakumari et al. 2011
		Wheat	0.87 (control) - 0.84 (drought stress)	Dhanda et al. 2004
		Soybean	0.69	Ao et al. 2010
		Rice	0.64	MacMillan et al. 2006
		Medicago truncatula	0.51 (control) - 0.44 (salt stress)	Arraouadi et al. 2011
		Wheat	0.41	Laperche et al. 2006
		Rice	0.41	Roy et al. 2009
Root length density / kinetics	Ratio length of root system to surface area of rhizotrons (cm cm^{-2})	Chickpea	0.14 - 0.57 depending on season and rooting depth	Kashiwagi et al. 2005
Depth of root system / kinetics	Maximum vertical depth of whole root system (cm)	Soybean	0.53	Ao et al. 2010
		Chickpea	0.36	Kashiwagi et al. 2005
Width of root system / kinetics	Maximum horizontal width of whole root system (cm)	Soybean	0.62	Ao et al. 2010
Angle of shoot borne roots	Angle between the horizontal and shoot borne roots (°)	Sorghum	0.47	Singh et al. 2011
Branching angle of lateral roots	Angle between main and branched lateral roots (°)			

Figures

Fig. 1: GROWSCREEN-Rhizo, mechanical setup with 72 positions for rhizotrons which are aligned in two rows in the greenhouse. The inclination angle of the rhizotrons is adjusted to 43° with transparent plate of the rhizotrons facing downwards. The rhizotrons are split into four groups which can be treated separately. The insert picture (top left) shows the irrigation system exemplary of one rhizotron with four drippers (A) to ensure a homogeneous distribution of water or nutrient solution over the rhizotron. To prevent light from reaching roots and also algal growth in the soil, the transparent side of the rhizotrons is shielded by an opaque plate (B) combined with dense, black brush curtains (C, insert picture top right). Between both rows of rhizotrons a cabinet (D) is moved automatically on a linear axis with bi-directional motion (indicated by white dashed arrow) to the positions of the rhizotrons. In a user defined order, the rhizotrons were drawn inside the cabinet for image acquisition of roots and shoots. The whole procedure is automated.

Fig. 2: Representative original and colour-coded images with main roots (in green) and lateral roots (in red) of an *Arabidopsis* (A, B) and *H. vulgare* cv. Barke (C, D) plant grown in soil-filled rhizotrons. The higher resolution image (E) shows an area of interest – indicated in (C) – with 5x magnification.

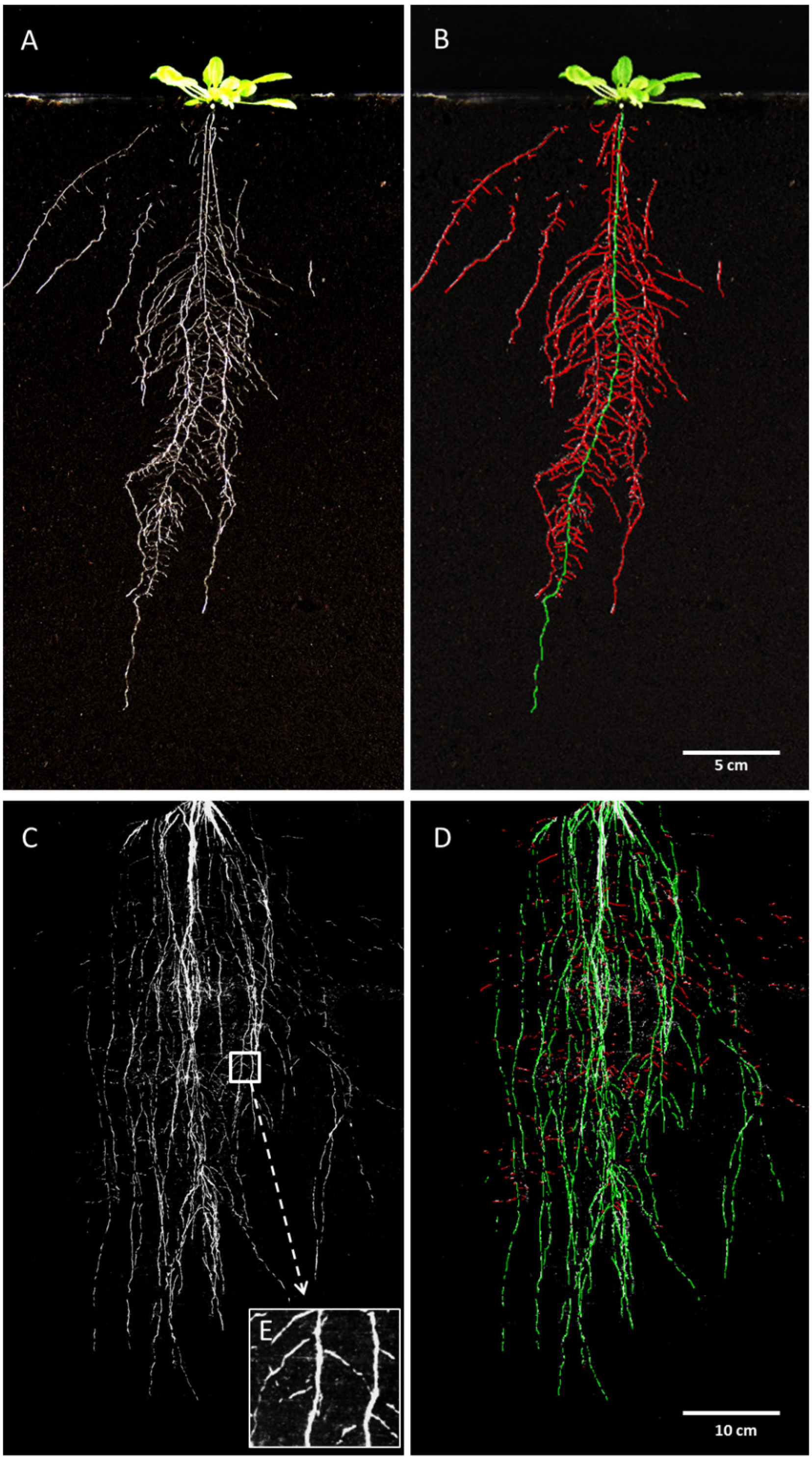

Fig. 3: Validation of root analysis software. Correlation between length of reference objects analysed with the software GROWSCREEN-Root and real length.

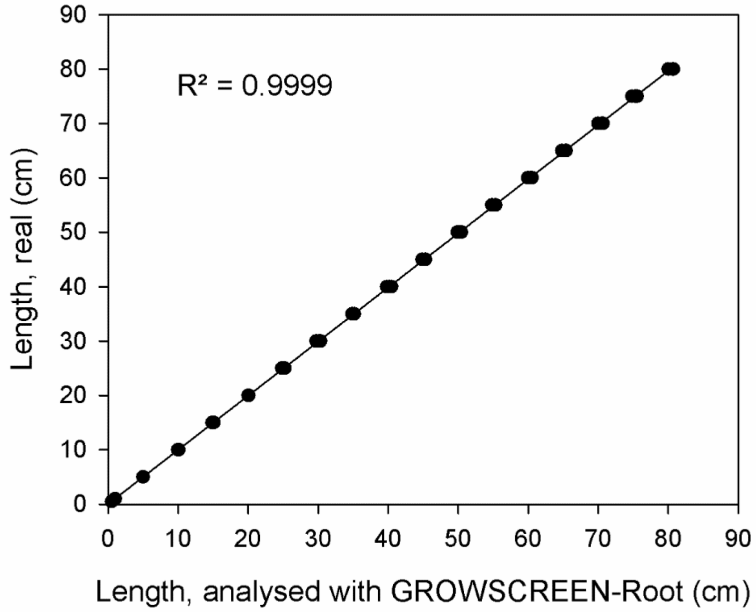

Fig. 4 Spatial distribution of roots visible at the transparent surface of soil-filled rhizotrons analysed with GROWSCREEN-Root. Root length density distribution of two model species, *Arabidopsis* and *Brachypodium* (A) and two crop species, *B. napus* (rapeseed) and *H.* vulgare cv. Barke (barley, B) was compared at equal root system length (approx. 260 cm). Plants were grown at a soil compaction level of approx. 0.07 MPa and rhizotrons were set to an inclination angle of 43° (mean value +/- SE, n=4-5).

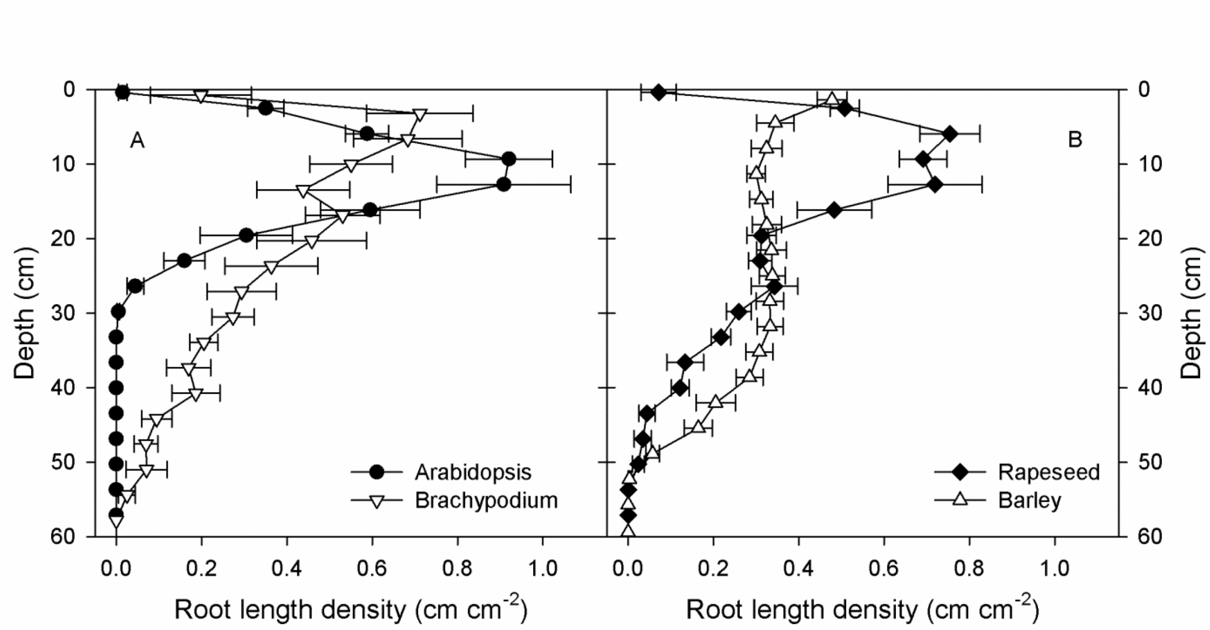

Fig. 5: Validation of leaf area analysis of *H.* vulgare cv. Barke (A, C) and *Zea mays* cv. Helix (B, D) plant. Correlation between the sum of projected leaf area analysed by taken images from two side-faces taken at a 90° horizontal rotation and the leaf area quantified by scanning the leaves (A, B) or fresh weight of shoots (C, D) was performed for 100 barley and 80 maize plants.

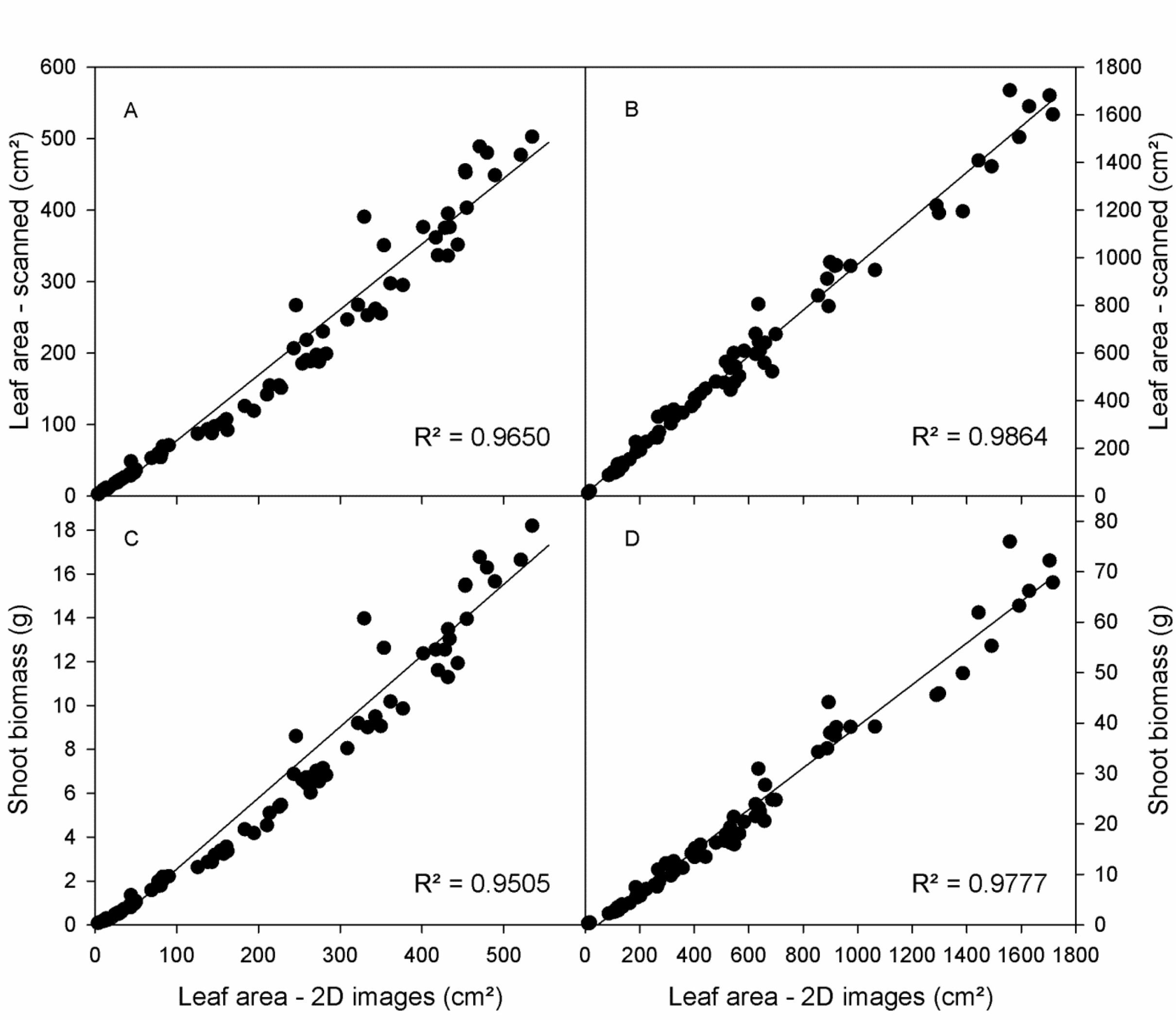

Fig. 6: Correlation between root length visible at the transparent surface of soil-filled rhizotrons with total root system length (A), root (B) and shoot (C) biomass as well as leaf area (D) of *Arabidopsis* (n=14), *Brachypodium* (n=14), *B. napus* (rapeseed, n=19), *H.* vulgare cv. Barke (barley, n=23), *O. sativa* (rice, n=30) and *Z. mays* (maize, n=21) plants grown in rhizotrons. Plants were grown at a soil compaction level of approx. 0.07 MPa and rhizotrons were set to an inclination angle of 43°.

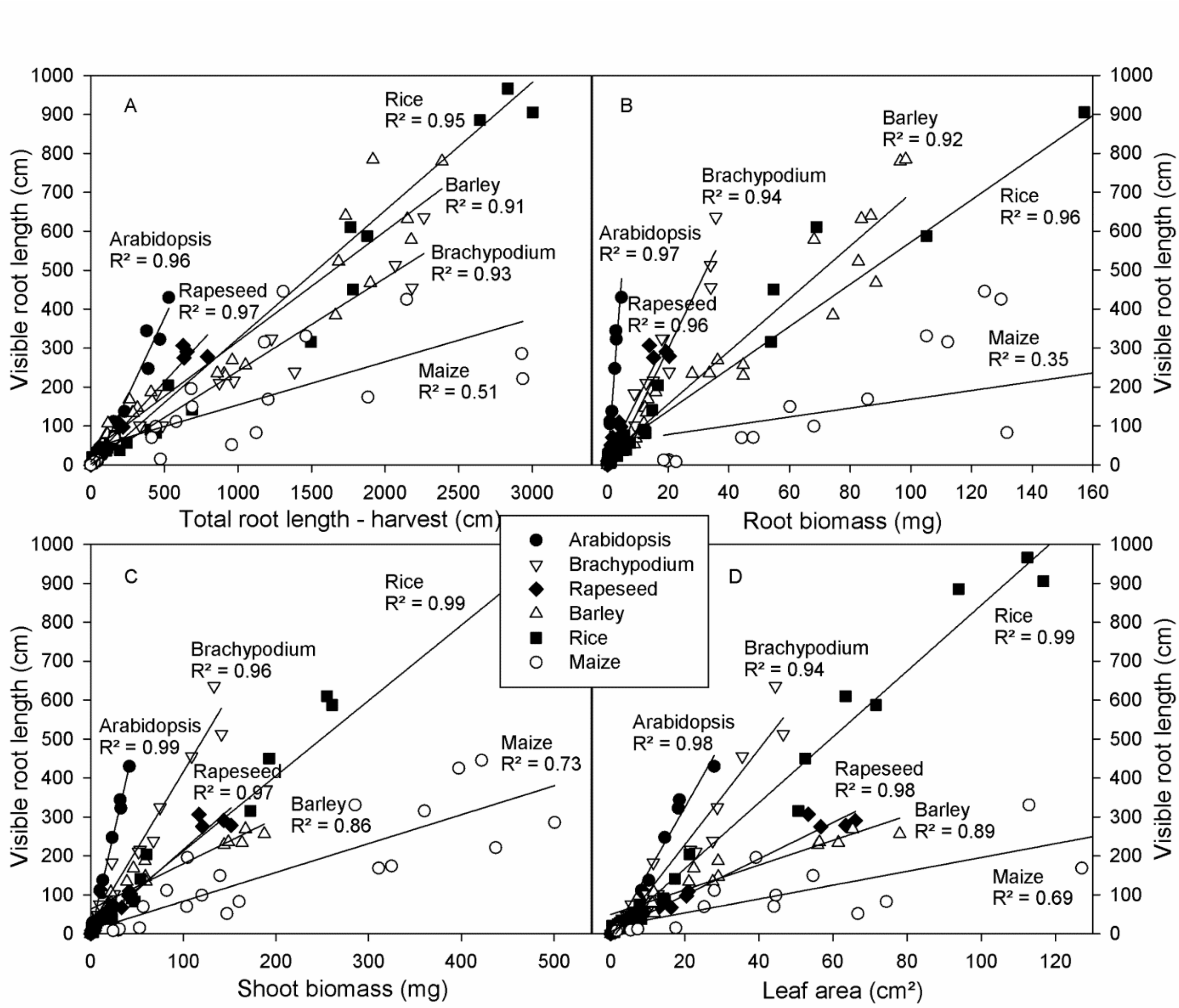

Fig. 7: Effect of mechanical impedance on root growth of *H. vulgare* cv. Golden Promise plants grown at two different soil compaction levels (0.06 MPa (low compaction) and 0.52 MPa (moderate compaction)) in rhizotrons (inclination angle of rhizotrons 43°). Soil compaction showed no effect on leaf area development (A), but affected main (B) as well as lateral (C) root growth and spatial distribution of roots (D), respectively. The results show the potential of the new device GROWSCREEN-Rhizo in quantifying dynamical changes of root growth and phenotyping root system architecture (mean value +/- SE, n=8).